ELECTRO-VORTEX FLOWS IN SHALLOW LIQUID METAL LAYERS

I. Kolesnichenko[1], *S. Khripchenko*[1], *D. Buchenau*[2], *G. Gerbeth*[2]

[1] *Institute of Continuous Media Mechanics, 1 Korolyov str., 614013 Perm, Russia (klsnchnk@icmm.ru)*
[2] *Forschungszentrum Rossendorf, MHD Department, Bautzner Landstraße 128, 01328 Dresden, Germany*

Introduction. The object of the present study is a vortex flow in a thin layer of a conducting fluid generated by an electromagnetic (EM) force. We consider a special version of em-forces, namely, the interaction of an externally applied electric current with its own magnetic field. We study this flow-driving action by considering a simple flat layer 1 (Fig. 1*a*, *b*) which has the form of a rectangular parallelepiped, the thickness d_0 of which is much less than its sizes a_0 and b_0 in the horizontal plane. A direct electric current I_0 with uniform density $\mathbf{j} = (j_x, 0, 0)$, where $j_x = I_0/b_0 d_0$, passes through the fluid layer between vertical walls. Its own magnetic field of induction $\mathbf{B}$ is enhanced by ferromagnetic yokes 2 with a jumper 3. The electromagnetic force $\mathbf{f}^{\rm em} = (0, -j_x B_z, 0)$ is rotational due to the restriction of the yoke sizes in the plane and, therefore, generates an electro-vortex flow (EVF) in the layer with one (Type A) or two (Type B) primary eddies (sketched in Fig. 1*a*) which may be unstable. We investigate the stationary state and oscillations of the EVF by experimental and numerical methods. In experiment we have employed the Ultrasound Doppler Velocimetry (UDV). With this non-invasive technique we can gain detailed information about the EVF, which can be readily processed and compared with numerical results.

1. Experimental setup. We studied the EVF in a plane quadratic layer *1* (Fig. 1*b*) of liquid metal (gallium alloy: $20.5\%\mathrm{In} + 67\%\mathrm{Ga} + 12.5\%\mathrm{Sn}$, $\rho = 6256\,\mathrm{kg/m^3}$ – density, $\nu = 3.1 \cdot 10^{-7}\,\mathrm{m^2/s}$ – kinematic viscosity, $\sigma = 3.56 \cdot 10^6\,\mathrm{S/m}$ – electrical conductivity) with thickness $d_0 = 0.01\,\mathrm{m}$ and sizes $a_0 = b_0 = 0.1\,\mathrm{m}$. The layer was bounded by vertical walls: one pair of opposite walls *5* was made of copper and played the role of electrodes, another pair of opposite walls *6* was made of plexiglas as well as the bottom *7* and the lid *8* (not shown in Fig. 1*b*). The direct electrical current source providing the current in the range of $I_0 = 0 \div 1100\,\mathrm{A}$ was

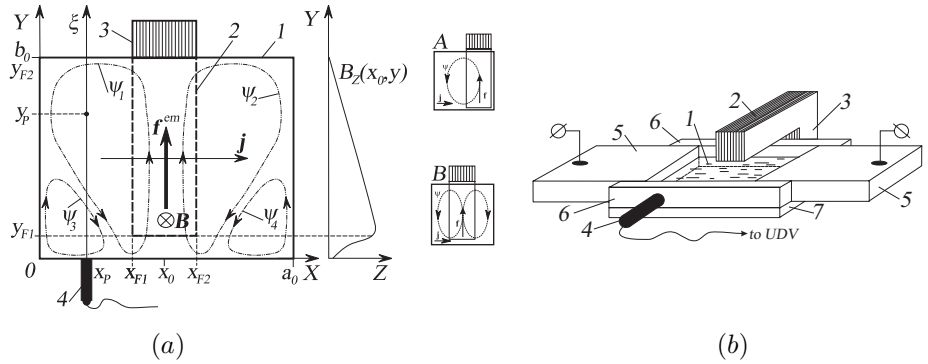

(*a*) (*b*)

Fig. 1. (*a*) Sketch of the MHD-layer (top view). (*b*) Scheme of the experimental setup without lid.

connected through feed wires with electrodes 5. The use of ferromagnetic yokes *2* ensures variation of the magnetic field of the electric current increasing the value of the field in the gap of $\delta = 0.03\,\mathrm{m}$ between the yokes. The yokes had the sizes $a_F = x_{F2} - x_{F1} = 0.03\,\mathrm{m}$, $b_F = y_{F2} - y_{F1} = 0.15\,\mathrm{m}$ (see Fig. 1*a*) and the jumper *3*. The use of this "C-core" allowed generation of the EVF with one or two primary eddies. The maximal local value of the magnetic field $B_0 = I_0\mu_0/\delta = 0.044\,\mathrm{T}$ was achieved at the C-core position $y_{F2} = 0$ for the current $I_0 = 1100\,\mathrm{A}$ (where $\mu_0 = 4\pi \cdot 10^{-7}\,\mathrm{H/m}$ is the vacuum permeability). To measure the velocity field, we employed the UDV "DOP2000" with a focused 4 MHz transducer *4* (Figs. 1*a*, *b*) of 8 mm diameter "TR30405" (Signal Processing SA, Lausanne, Switzerland). We directed the US beam normally to the walls *6* as this direction provided the spanwise velocity component. During each UDV measurement we obtained a sequence of N^{pr} velocity profiles $U(x_P, y^{\mathrm{pr}}, t^{\mathrm{pr}})$ along the axis ξ (Fig. 1*a*). Here x_P is the position of the US transducer *4* (we used $x_P = \{5; 10; ..90; 95\}$ mm), y^{pr} is the vector of N_y points along ξ (we used $N_y = 304$), t^{pr} is the vector of N_t points on the time axis (we used $N_t = \{512; 1024; 4096\}$). Fig. 2*a* shows one of the profiles from the obtained sequence at some fixed time moment t^*. Due to multiple reflections, the profile in the regions near walls I and II is not directly accessible (but actually, the value at the bottom has to be zero because of the "non-leakage" condition). To take into account the "shadow"-effect caused by local losses of the signal (IV in Fig. 1*a*), we applied a "rejecting zero" procedure.

2. Mathematical model. To formulate the mathematical model describing the electro-vortex flow of laminar and turbulent nature observed during experiments, we have used a system of MHD equations resulting from a suitable reduction of the problem complexity. We first use the low magnetic Reynolds number assumption $\mathrm{Rm} \ll \delta/a_0$. With this approximation, one can ignore the influence of the flow on the electromagnetic field. In our case, $\mathrm{Rm} = \mu_0\sigma V_0 d_0 = 0.044 V_0$ and $\delta/a_0 = 0.3$, so that this approach was appropriate for our treatment up to a maximal velocity of $V_0 < 1$ m/s. Therefore, we can calculate the electromagnetic force density $\mathbf{f}^{\mathrm{em}}$ using the electric current j_x and the induction B_z [1] only. Another approximation, which can be applied to thin layers $d_0 \ll min(a_0, b_0)$, is based on an assumption that the velocity field vector has no vertical component. We approximate the horizontal velocity components $V_i^{3D}(x, y, z, t) = V_i(x, y, t) f_V(z, \mathrm{Ha}, \mathrm{Re})$ by multiplying the planar velocities V_i by a function f_V, which describes the ver-

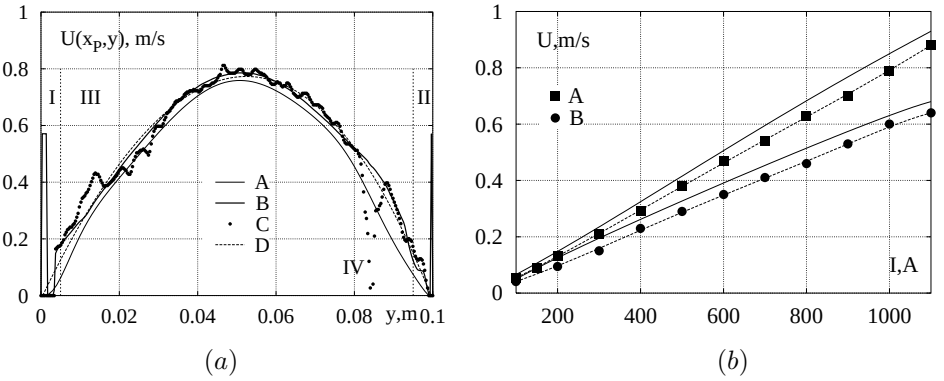

Fig. 2. (*a*) Example of velocity profiles ($I_0 = 1000$ A, Type A): A – calculated profile $V_y(x_P, y, t^*)$, B – mean of $N_t = 512$ experimental profiles $\overline{U}(x_P, y)$, C – instantaneous experimental profile $U(x_P, y, t^*)$, D – approximation of U by Chebyshev polynomials (U^{appr}). (*b*) Maximum mean velocity vs. the electric current (here and after A – for the EVF of type A, B – for the EVF of type B, solid lines – calculations).

tical profiles ($i = 1, 2$ with the notation $V_1 \equiv V_x$, $x_1 \equiv x$,...), where $\mathrm{Re} = V_i$ is the Reynolds number and $\mathrm{Ha} = B_0 B_z d_0 \sqrt{\sigma/\rho\nu}$ is the Hartmann number. In our case these numbers have the following maximum values: $\mathrm{Re} \leq 3.3 \cdot 10^4$, $\mathrm{Ha} \leq 34$. It means that the flow may be turbulent, and the magnetic field may influence the flow structure and the instability threshold. Eventually, the Navier-Stokes equation for the incompressible flow $V_{i,i} = 0$, integrated along the vertical axis through the layer, for $i, j = \{1, 2\}$ is written as

$$\frac{\partial V_i}{\partial t} + V_j \frac{\partial V_i}{\partial x_j} = -\frac{\partial (P + k^{\mathrm{T}})}{\partial x_i} + \nu^{\mathrm{T}} \frac{\partial^2 V_i}{\partial x_j^2} + \kappa V_i + \frac{\partial \nu^{\mathrm{T}}}{\partial x_j} e_{ij} + S f_i^{\mathrm{em}} \qquad (1)$$

Here we use the following notations: P is the pressure, k^{T} is the turbulent kinetic energy, $\nu^{\mathrm{T}} = (1 + \eta^{\mathrm{T}}/\rho\nu)$ is the turbulent kinematic viscosity which is defined using the k^{T}-ω^{T} model [2], κ is the factor describing the turbulent friction near the horizontal solid walls depending on the local Re and Ha numbers, $e_{ij} = V_{i,j} + V_{j,i}$ is the tensor of velocity deformation, and $\mathrm{S} = I_0^2 \mu_0 d_0 / \rho\nu^2 \delta$ is the parameter of MHD-interaction. At the solid side walls of the layer the no-slip condition for the velocity must be fulfilled: $V_i(x = \{0; a_0\}, y) = 0$, $V_i(x, y = \{0; b_0\}) = 0$.

3. Results. To analyze the experimentally and numerically obtained results, we have processed two types of information about the velocity fields: values of the velocity component at the selected point $U(x_P, y_P, t)$ (see Fig. 1*a*), and the velocity profiles $U(x_P, y_i, t)$ along the y-axis. Fig. 2*b* shows the dependence of the mean velocity $\overline{U}(x_P, y_P)$ on the electric current. It is seen that the larger the scale of eddies, the higher the velocity. As could be expected from Eq. (1), the maximum mean velocities increase linearly with the external current. A good agreement is seen between the experimental and theoretical results in Fig. 3. To construct the streamfunction, we have calculated the Chebyshev approximation $\overline{U}_M^{\mathrm{appr}}(x_P, y_i)$ (hereinafter the overscript bar denotes the time-averaging procedure) of velocity profiles obtained for the values of $x_p = j * 5\,\mathrm{mm}$ ($j = 1...19$) by moving the UDV sensor along the sidewall of the layer and integrated them along the x-axis (forward and backward averaging of the results of integration along the x-axis) $\psi(x_j, y_i) = 0.0025 \left(\sum_{k=0}^{j} U_M^{\mathrm{appr}}(x_k, y_i) - \sum_{k=j}^{20} U_M^{apr}(x_k, y_i) \right)$.

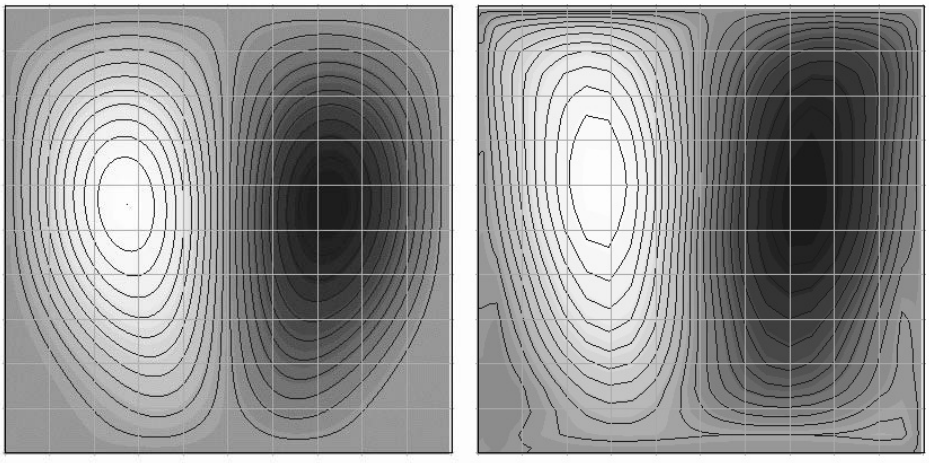

(*a*) (*b*)

Fig. 3. Example of stream-function ψ (the EVF of type B, $I_0 = 100$ A): (*a*) calculations, (*b*) experiment.

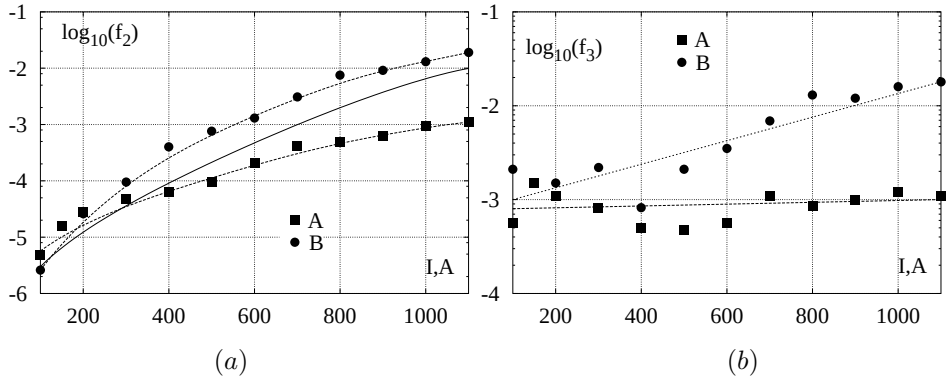

Fig. 4. (*a*) Energy f_2 of the measured velocity signals at the point (x_p, y_p) vs. the electric current: dots – experimental data for types A and B, solid line – calculations for type B. (*b*) Energy f_3 of the velocity profiles at $x = x_p$ vs. the electric current.

The growth of the external current I_0 leads to an increase of velocities and to a higher level of oscillations. Fig. 4*a* shows the energy $f_2 = \sum_k F_k^2$ of the signal $u'(t) = (U(x_P, y_P, t)/\overline{U}(x_P, y_P) - 1)$, where $F_k \equiv FT_k(u')$ is the Fourier-spectrum. One can see that the level of oscillations for the EVF of type B is higher than for type A, however, for both EVF types f_2 grows with increase of the electric current. Apart from the analysis of signal fluctuations at one point, it is also interesting to calculate the energy f_3 based on the velocity profile along the y-axis. We transform the functions $u'^*(x_P, y_i, t) \equiv U(x_P, y_i, t)/ < U(x_P, y_i, t) >$ which are the profiles divided by their coordinate-averaged value, and perform smoothing in terms of Chebyshev polynomials $u^*(t) = TT_m(u'^*)$, where $u^*(t)$ is the spectrum. Calculating for each external electric current the energy f_3 via $f_3 = \sum_k G_k^2$ where $G_k = FT_k(u^*)$, we obtain the results shown in Fig. 4*b*. As expected, smoothing with the Chebyshev spectrum procedure eliminates the short-wave components. These results are an obvious demonstration of the fact that in the present case the EVF with two-eddies is less stable than the EVF with one eddy. A close agreement between the theoretical and experimental results was obtained. Thus, the applied model proved to be capable of providing reliable data for this class of flow problems.

4. Acknowledgements. The research described in this publication was made possible in part by Awards No. YSF 2002-424 of the International Association for the promotion of cooperation with scientists from the New Independent States of the former Soviet Union (INTAS), and German "Deutsche Forschungsgemeinschaft" in frame of the Collaborative Research Centre SFB 609.

REFERENCES

1. I. Kolesnichenko, S. Khripchenko. Surface instability of the plane layer of conducting liquid. *Magnetohydrodynamics*, vol. 39 (2003), no. 4, pp. 427–434.

2. D. C. Wilcox. *Turbulence modeling for CFD* (DCW Industries, Inc. La Canada, California, 1993).